Cretaceous to Paleocene depositional history of North-Pacific subduction zone: reconstruction from the Nemuro Group, eastern Hokkaido, northern Japan

Hajime Naruse

Kyoto University, Graduate School of Science, Department of Geology and Mineralogy, Kitashirakawa-oiwakecho, Sakyo-ku, Kyoto 606-8502, Japan.

The Campanian to Paleocene Nemuro Group, the oldest strata in the Kuril Arc, is distributed in the east of Hokkaido Island, northern Japan. Strata of the group in this study area are sedimentologically classified into eight depositional facies, most of which are interpreted as sediment gravity flow deposits. These depositional facies comprise four depositional facies associations. The distal basin plain and proximal basin plain facies associations are composed mainly of hemipelagic mudstone and sandstones that are interpreted as sediment gravity flow deposits, and were deposited in a topographically flat environment inferred by good lateral continuity of lithofacies. The channel-levee complex and submarine slope facies associations, in contrast, are composed of hemipelagic mudstone, turbidites and debris flow deposits. These facies associations were deposited in a channel-levee complex environment. The distal basin plain, proximal basin plain, channel-levee complex

and submarine slope facies associations stack in ascending order, and represent a regressive succession. Palaeocurrent data indicate that the deposits of the Nemuro Group were transported from the northwest. Hence, the group in the study area is concluded to record slope progradation away from the northern source area. It was known that there was regression on the Kuril Arc based on the hiatus in the Eocene, and there was an interpretation that the regression to be attributable to ridge subduction beneath the Kuril Arc. This study revealed that regression in the Kuril Arc began as early as Maastrichtian. This may have been induced by volcanic activity in the Kuril Arc or a significant eustatic fall of sea level.

KEY WORDS: subduction zone; slope facies; Nemuro Group; Maastrichtian; North Pacific

1. Introduction

The Kuril island arc system is a typical subduction zone in the North Pacific (Figure 1). The Kuril Arc is important for investigating the tectonic models of island arcs (Kusunoki and Kimura, 1998) because it has experienced various tectonic events such as expansion of a back-arc basin (Kimura & Tamaki, 1986) and Miocene collision with the Tohoku Arc of northern Japan (Kusunoki & Kimura, 1998). However, pre-Tertiary tectonic history, regarded as the period immediately following the initiation of development of the Kuril Arc, has yet to be revealed in detail. To reconstruct the evolutionary processes for pertaining to the arc, information concerning its pre-Tertiary history is necessary.

The Campanian-Paleocene Nemuro Group, the oldest strata of the Kuril Arc, crops out in the east of Hokkaido Island, northern Japan. It is interpreted as a forearc basin deposit owing to the extensive volcaniclastic deposits and the distribution of the group parallel to the Kuril Arc (Figure 1). In Addition, the Nemuro Group exposed in the eastern coast area of the Hokkaido Island is hardly influenced by tectonic deforemation. Therefore, the Nemuro Group is considered to hold information vital to the understanding of the early geologic history of the Kuril Arc.

Kiminami (1983) proposed a hypothesis in which the sedimentary basin of the Nemuro Group had two different source areas: the northern continent and the southern volcanic arc, based mainly on sedimentary petrological evidence. Kimura & Tamaki (1986) suggested that the southward migration of the volcanic front, proposed as the southern source area by Kiminami (1983), was induced by the subduction of the active Kula-Pacific ridge beneath the Kuril Arc. Kimura & Tamaki (1986) also inferred that ridge subduction was also responsible for the sudden uplift of the sedimentary basin of the Nemuro Group. However, there is as yet insufficient sedimentological data to suggest the existence of the southern volcanic island arc, and the detailed depositional history of the Nemuro Group remains unclear.

In the present paper, a detailed depositional history of the Nemuro Group is presented based on depositional facies analysis. The proposed history provides reasonable constraints on the tectonic history of the Kuril Arc during the Late Cretaceous-Paleocene.

2. Geologic setting

The Cretaceous-Paleocene Nemuro Group is a marine clastic sequence, about 3000 m thick, mainly composed of hemipelagic mudstone, turbidites, and submarine slump deposits (Kiminami, 1978). The group is extensively exposed along coastal cliffs in the Hamanaka-Nemuro area (Figure 1), while outcrops are sparse further inland. Although the lower strata are not exposed, up to 2000 m of the sequence can be directly observed in the study area. The group is unconformably overlain by the Eocene Urahoro

Group. Bedding strikes 60°-80° north and dips 10°-20° to the south (Figure 2). Distinct tectonic folding was not observed.

The Nemuro Group consists primarily of sediment gravity flow deposits and hemipelagic mudstones. Submarine slump deposits are particularly abundant in this area. Several sills of mafic igneous rocks and acidic tuff beds are present, and most sedimentary rocks contain clasts derived from igneous rocks (Kiminami, 1979). The group is subdivided in the area into five formations (Monshizu, Oborogawa, Hamanaka, Akkeshi, and Kiritappu in ascending stratigraphic order), and the stratigraphic contact between the formations are conformable. The upper four formations are discussed in detail here.

The Oborogawa Formation (Nagao, 1957) comformably overlies the Monshizu Formation, and is about 190 m thick. It consists mainly of dark grey mudstone and several beds of acidic tuff.

The Hamanaka Formation (Kiminami, 1978) conformably overlies the Oborogawa Formation. It is 200-250 m thick, and is sandstone-dominated, comprising alternating beds of sandstone and mudstone. A characteristic acidic tuff bed, 2 m thick, is observed in the lowermost part of the Hamanaka Formation.

The Akkeshi Formation (Nagao, 1957) conformably overlies the Hamanaka Formation, and is 900-1300 m thick. It consists mainly of alternating thinly bedded (less than 15 cm thick) or laminated fine sandstone and mudstone, thickly bedded or structureless poorly sorted coarse sandstone, and chaotic deposits (Pickering *et al.*, 1989). The chaotic deposits consist of contorted blocks of sedimentary and igneous rocks with a gravelly mudstone matrix.

The Kiritappu Formation (Yoshida, 1967) conformably overlies the Akkeshi Formation. It is the uppermost formation in this study area, and more than 250 m thick. It consists of pebble to cobble conglomerates and bioturbated sandy siltstone.

The Nemuro Group ranges from the Campanian to the Paleocene in age, and the Cretaceous/Paleogene boundary was thought by Naruse et al. (2000) to occur within the upper part of the Akkeshi

Formation, who suggested that the succession from the Oborogawa Formation to the middle Akkeshi Formation is of early Maastrichtian age according to megafossil biostratigraphy. Okada *et al.* (1987) suggested, on the basis of calcareous nannofossil biostratigraphy, that the upper Akkeshi Formation is referable to the Danian (Paleocene). Yoshida (1967) also suggested, based on planktonic foraminiferal biostratigraphy, that the Kiritappu Formation is Paleocene in age.

3. Depositional facies

Strata of the Nemuro Group in the study-area are sedimentologically classified into eight depositional facies based on bed shape, thickness, grain-size distribution, and internal sedimentary structures (Figure 4). The differences in the characteristic features of each facies are considered to reflect differing depositional processes. Most facies are interpreted as sediment gravity flow deposits, with the exception of Facies 1-a and 1-b as discussed below.

Facies 1-a: laminated mudstone

Description. This facies 1-a is primarily composed of dark grey mudstone intercalated with thin (less than 5 mm thick) sandstone laminae. The mudstone is nearly homogeneous or weakly bioturbated, and sand grains are rare. Small horizontal burrows of *Phycosiphon* isp., and *Scalarituba* isp. are observable. These ichnofossils are less than 4 mm in diameter. Macrofossils occur very rarely in this facies.

Interpretation. This facies is interpreted as hemipelagite or mudstone deposited directly from suspension load of low-density turbidity current because the mudstone lacks any structures indicative of gravity flows, waves, or currents. The sandstone laminae may be distal turbidites or contourites. It is difficult to distinguish turbidite mudstones or turbidite sandstone laminae from hemipelagites or contourites because this facies is bioturbated.

Facies 1-b: bioturbated sandy siltstone

Description. Facies 1-b is composed of intensely bioturbated siltstone containing sand-sized particles. Smooth concave-upward erosional surfaces are often observed in the mudstone (Figure 5A), ranging from approximately 5 to 100 m in width and filled with fine deposits.

Fossils of molluscs (the bivalves *Periploma* sp., and *Acila* sp., gastropods and scaphopods) are commonly found in this facies.

Interpretation. The siltstone of facies 1-b is interpreted as a deposit sourced from hemipelagite or suspended load of low-density turbidity current similar to facies 1-a. Sand grains may have been transported by sediment gravity flows or storm-generated flows. However, any primary sedimentary structures are lost and this facies was mixed with silts as a result of intense bioturbation.

The listric erosional surfaces are interpreted as slump scars. Such features are frequently observed in the upper part of modern submarine slopes, and are distinguished by their smooth concave-upwards erosional form, filled with fine-grained deposits (Clari & Ghibaudo, 1979; Postma, 1984).

Facies 2-a: thinly bedded fine-grained sandstone

Description. Facies 2-a is a graded fine-grained sandstone bed. Beds are less than 0.2 m in thickness, and are typically graded from fine sand to coarse silt (Figure 5B). Parallel lamination is common, but cross lamination is very rare. Bottom surfaces are usually flat.

Interpretation. Facies 2-A is interpreted as a turbidite. Graded bedding, which is common in this facies, is a typical feature of turbidites (Middleton & Hampton, 1976). The parallel laminated sandstone observed in this facies correspond to the

T_b division of a Bouma sequence (Bouma, 1962). The absence of particles coarser than medium-grained sand and the lack of a structureless graded sand division (Bouma's T_a division) suggest that sandstone beds of this facies were deposited from low-density turbidity currents (Middleton & Hampton, 1976; Lowe, 1982). All sandstone beds are thin, and flute casts suggesting the existence of intense turbulence in flows (Walker, 1978, 1985) are rare.

Facies 2-b: thinly bedded laminated sandstone

Description. Facies 2-b is a thinly bedded graded sandstone facies composed of grains less than medium sand in size. Most beds range from 5 to 15 cm in thickness (80 cm maximum). Sandstone beds commonly exhibit parallel, climbing-ripple, and convolute lamination (Figure 5C). Many flute casts can be observed on the bottom surface of the sandstone beds (Figure 5D).

This facies consists of two divisions. Division 1 consists of graded medium to very fine-grained sandstone with parallel lamination. Division 2 is composed of fine-grained sandstone to coarse siltstone displaying climbing ripple cross-lamination or convolute lamination. Climbing ripple cross-lamination often grades into convolute lamination.

Interpretation. Sandstone beds of this facies are similar to those of Facies 2-a, which is interpreted as a low-density turbidite. This facies exhibits grading, lacks coarse sand. These characteristics are typical of low-density turbidites (Middleton & Hampton, 1976; Lowe, 1982), and suggest that Division 1 of this facies corresponds to Bouma's T_b division and Division 2 can be classified as the T_c division (Bouma, 1962; Walker, 1978).

Abundant climbing ripple cross-lamination in the turbidite is indicative of a high suspension fall-out rate (Allen, 1971). Convolute laminations suggest that shear stress as a result of sediment gravity flow was high (Walker, 1992). The abundance of flute casts on the bottom surfaces of the sandstone beds implies turbulence in the flow (Sanders, 1965). These features all suggest that the intensity of the turbidity current in this facies was higher than Facies 2-a, although the flow itself consisted primarily of fine sediment as suspended load.

Facies 3-a: structureless coarse sandstone

Description. Facies 3-a is represented by poorly sorted structureless coarse sandstone bed that includes granules and large (maximum 50 cm in thickness, 3 m in length) deformed mud clasts (Figure 5E). The beds range from 0.3 to 3 m in thickness. They usually extend laterally with uniform thickness. For Example, one bed belonging to this facies changes its thickness in only 12% between two outcrops correlated by a characteristic tuff bed although they are 6 km apart from each other (Figure 7). Many groove casts are observed on the bottom surface of this facies.

Facies 3-a is subdivided into divisions 1 - 3 that differ in terms of grain size and sedimentary structures (Figures 4). Facies 3-a is typically composed of divisions 1- 3, but some beds lack 1 or 3.

Division 1 forms the lowest part of the bed. It is less than 20 cm thick, consists of coarse sandstone with granules, and often exhibits inverse grading (Figure 5E). Division 2 represents the mid section of a bed. It ranges from 0.2 to 3 m in thickness and consists of poorly sorted coarse sandstone with granules. This division is almost structureless, and includes mud clasts and deformed blocks of alternating beds of sandstone and mudstone (Figure 5E). Most sandstone beds included in this division as clasts exhibit the features of Facies 2-b. Division 3 is the uppermost part of the bed. It is less than 30 cm thick, consists of medium sandstone to coarse siltstone, and exhibits parallel laminations. Climbing ripple cross-lamination occurs rarely. This division is graded and passes up into mudstone (Facies 1-a).

Interpretation. Facies 3-a is interpreted as a sediment gravity flow deposit (Lowe, 1982; Mulder & Alexander, 2001). The sediment gravity flow that deposited this facies is inferred to have had a high particle concentration (Shanmugam, 1996; Kneller & Buckee, 2000; Mulder & Alexander, 2001) because this facies include particles coarser than coarse sand and grain-supporting mechanisms related to the particle concentration (dispersive pressure, buoyancy, matrix cohesion) are necessary to transport such particles coarser than medium sand (Lowe, 1982).

This facies includes three divisions with differing sedimentary features, suggesting that the depositional processes in the high-concentration sediment gravity flow varied over the period of deposition. Division 1 exhibits inverse grading ranging upward from medium-grained sandstone to granules, and is less than 15 cm in thickness. It is consistent with deposition from a traction carpet (Lowe, 1982; Sohn, 1997). A inverse-graded granule layer called a traction carpet deposits (Lowe, 1982) or spaced stratification (Hiscott & Middleton, 1979) is a common sedimentary structure in coarse-grained gravity flows, pyroclastic flows and surges, and subaerial hyperconcentrated flow deposits. The origin of the inverse grading is, however, still unknown (Sohn, 1997). Division 1 corresponds to Lowe's S_2 division (Lowe, 1982).

The structureless feature of Division 2 suggests that this division was deposited by direct suspension sedimentation (Lowe, 1982) or frictional freezing (Shanmugam, 1996). The abundance of coarse grains in this division suggests that the flow had high particle concentration. Division 2 is similar to Bouma's T_a and Lowe's S3 divisions.

Division 3 is interpreted as a deposit originating from traction sedimentation of turbidity currents, and is classfied as Bouma's Tb division. Grading, one of the general features of turbidites (Bouma, 1962), is also well defined in this division. Parallel lamination, which is evidence of traction sedimentation, of this division suggests that the flow had evolved to a low-density turbidity current (Lowe, 1982).

To summarize the features of divisions 1-3, this facies was transported by sediment gravity flows that possessed a high particle concentration, rapidly evolving to a low-density turbidity current (Lowe, 1982).

Facies 3-b: Thickly bedded pebbly sandstone

Description. Facies 3-b is a poorly sorted pebbly coarse sandstone bed (Figure 6A) that ranges from 30 cm to 10 m in thickness. Many mud clasts of less than 10 cm in diameter are included in this facies. The facies overlies mudstone with an irregular erosional surface.

This facies is subdivided into divisions 1-3 based on grain size and sedimentary structures. The typical section consists of these divisions in ascending order, but many beds of this facies lack 1 and 3.

Division 1 consists of coarse sandstone with granules, and ranges from 0.1 to 0.3 m in thickness. One or several inverse graded layers are often observable. Division 2 is structureless to slightly graded and consists of poorly sorted pebbly coarse sandstone. No laminations are observed. It ranges from 0.3 to 10 m in thickness. Division 3 is composed mainly of medium to coarse sandstone, graded upward into structureless mudstone. It ranges from 10 cm to 1.5 m in thickness and exhibits parallel and/or large-scale cross-bedding (set height is more than 20 cm, Figure 6B).

Interpretation. Facies 3-b is interpreted as a sediment gravity flow deposit (Lowe, 1982), similar in many respects to Facies 3-a. Grading, a characteristic feature of turbidites, is common in this facies. Abundant granules and very coarse sands in this facies suggest that this facies is deposited from the sediment gravity flow that had a high particle concentration, because transportation of coarse sediments needs grain-supporting mechanisms related to the particle concentration (i.e. dispersive pressure, buoyancy and matrix cohesion) (Middleton and Hampton, 1976; Lowe, 1982). Erosional features and flute marks on the bottom surface suggest that the sediment gravity flow was more turbulent and powerful (Lowe, 1982) than that forming Facies 3-a.

The three different divisions observed in this facies suggest that the depositional processes changed over the period of deposition. Division 1 is interpreted to have been deposited from a "traction carpet" (Lowe, 1982), similar to Division 1 of Facies 3-b, on the basis of its inverse grading. Division 2 is though to have been deposited rapidly by direct suspension sedimentation (Lowe, 1982), as indicated by its structureless form. This is similar to Bouma's T_a and Lowe's S_3 division (Bouma, 1962; Lowe, 1982). Parallel laminations and large-scale cross stratification included in Division 3 indicate that this facies component was deposited by traction sedimentation.

An exceptional feature of this facies is the development of cross-stratification, which is very rare in turbidites, although Similar large-scale bedforms are frequently observed in modern submarine channels.

Facies 3-c: graded conglomerate

Description. Facies 3-c is composed of subrounded pebble to cobble conglomerate and pebbly coarse sandstone (Figure 6C). The beds range from 0.3 to 10 m in thickness, with irregular erosional surfaces at the base. These beds are frequently amalgamated and form thick conglomerate sections of up to approximately 50 meters thick.

This facies is subdivided into divisions 1-3 based on grain-size and sedimentary structures. The typical succession consists of three divisions in ascending order, but many beds lack 1 and 3. Division 1 is a clast-supported granule to cobble conglomerate ranging from 0.1 to 1 m in thickness. Inverse grading is a characteristic feature of this division. Gravels in this division are not imbricated. Division 2 is a clast-supported pebble to cobble conglomerate ranging from 0.5 to 6 m in thickness and exhibits weak normal grading. Gravels in this division are usually imbricated. Division 3 is mainly composed of poorly sorted structureless pebbly sandstone ranging from 0.1 to 0.5 m in thickness. Some cobbles are included as floating components in the pebbly sandstone of this division.

Interpretation. Facies 3-c is interpreted as a gravelly sediment gravity flow deposit. It is inferred that this facies was deposited from a high-concentration turbidity current (Lowe, 1982; Mulder & Alexander, 2001) or inertia debris flow (Takahashi, 2001). With the exception of the lowermost Division 1, this facies exhibits normal grading and a succession of internal sedimentary structures and fabrics that contrast with those of cohesive debris-flow deposits (Facies 4).

The fact that this facies is composed of three divisions indicates that the depositional processes evolved during sediment gravity flow. The inverse grading of Division 1 indicates that dispersive pressure resulting from clast collisions (Bagnold, 1954; Sohn, 1997) was an effective grain support mechanism during that period (Shanmugam, 1996; Mulder & Alexander, 2001). This division is equivalent to Lowe's R_2 division. Division 2 is composed of graded conglomerates that accumulated beneath turbidity currents or inertia debris flows in which dispersive pressure was not effective. This division is equivalent to Lowe's R_3 division. After rapid settling or freezing of the gravels, residual sandy sediments probably settled gradually and formed Division 3. It is suggested that most of the sandy sediments were transported downflow because division is thinner than the others. It is equivalent to Bouma's T_a or Lowe's S_3 division.

Facies 4 chaotic deposits

Description. Facies 4 is composed of poorly sorted pebbly mudstone and deformed blocks (Figure 6D). It ranges from 50 cm to more than 100 m in thickness. The blocks range from 1 to 10 m in diameter, but a few huge blocks of more than 100 m in diameter are observed. They mainly consist of thickly bedded pebbly sandstone (Facies 3-b) or alternating mudstone (Facies 1-a) and thinly bedded sandstone (Facies 2-b). They occur dispersed in the pebbly mudstone matrix, and do not exhibit preferred orientation. They are rarely in direct contact with each other. Neither normal nor inverse grading is observable in this facies.

Interpretation. This facies is interpreted as a cohesive debris-flow deposit (Johnson, 1970; Lowe, 1979). Since inverse grading is not observed, it is inferred that dispersive pressure resulting from grain collisions was not an important grain support mechanism. The blocks are considered to have been supported by matrix cohesion (Johnson, 1970), as indicated by the floating nature of these blocks in the matrix. It is implied that the sediment gravity flow transporting such blocks froze (Middleton & Hampton, 1976). Generally, cohesive debris flows (Lowe, 1979), in which particles are supported by buoyancy and matrix cohesion, stop suddenly when the shear stress becomes lower than the internal matrix strength.

Since most chaotic beds in this facies are very thick (up to more than 100 m), it is considered that the mass flows resulted from large slope failures.

4. Depositional environments

Four facies associations are identified based on the included facies, the pattern of stacking, and the lateral continuity of successions. The Oborogawa, Hamanaka, Akkeshi, and Kiritappu formations represent distal basin plain, proximal basin plain, channel-levee complex and submarine slope facies associations, respectively.

Distal basin plain facies association (Oborogawa Formation)

The distal basin plain facies association consists mainly of Facies 1-a and Facies 2-a (Figure 4). Based on observation of the outcrops (usually 50-200m in width), the beds are laterally continuous, and neither slump scars nor other erosional structures are observed. This facies association shows a gradual upward-coarsening succession. Current-ripple laminations and sole marks indicate a north to south palaeocurrent direction.

Good lateral continuity of the lithofacies suggests that this facies association was deposited in a topographically flat environment in a distal basin plain. There is no evidence of depositional slope, and the facies association includes only distal turbidites (Facies 2-a) and hemipelagic mudstone (Facies 1-a). These features suggest that this formation was deposited in a distal area of a basin plain (Walker, 1978).

Proximal basin plain facies association (Hamanaka Formation)

This facies association consists mainly of Facies 1-a, 2-a, and 3-a (Figure 4); Facies 4 is rarely observed in this association. The facies are interpreted as deep-sea deposits consisting of hemipelagic mudstone (Facies 1-a), low-density turbidites (2-a), highly concentrated sediment gravity flow deposits (3-a), and debris flow deposits (Facies 4). Highly concentrated sediment gravity flow deposits (facies 3-a) has well-developed structureless division (Division 2), and includes many large mud and sand clasts, suggesting that this facies was deposited relatively proximal to a basin plain.

The beds are laterally continuous, and several sandstone beds (facies 2-a and 3-a) can be traced for more than 10 km (Figure 7). Evidence indicative of a slope environment is rare. Therefore, this facies association appears to represent a topologically flat depositional environment.

Palaeocurrent data from cross-laminations and sole marks are concentrated, indicating that almost all deposits were transported from the northern area (Figure 8).

Compared to the distal basin plain facies association, coarse-grained sediment gravity flow deposits (Facies 3-a) are more abundance in the proximal basin plain facies association.

Channel-levee complex facies association (Akkeshi Formation)

This facies association is mainly composed of extensive large-scale debris-flow deposits (Facies 4). Especially in the Eastern Nemuro Area (Figure 2I), Almost all outcrops of the Akkeshi Formation consist of debris-flow deposits. Those debris-flow deposits often include huge sedimentary rock blocks (10-100m in diameter), and lithologies of those blocks can be classified into successions A and B. Primary relationship between successions A and B can be observed in the outcrops of the western part of the study area, where slump deposits are not developed (Figure 2III; Figure 9).

Succession A exhibits an upward-thinning succession composed of pebbly sandstone beds (Facies 3-b) and chaotic deposits (Facies 4; Figure 9). These deposits originate from coarse-grained sediment gravity flows such as high-density turbidity currents (Facies 3-b) and cohesive debris flows (Facies 4). Upward-thinning successions are represented, being typical of channel-fill deposits (Walker, 1978, 1992). Strikes and dips of Succession A show gradual change laterally and also suggest its channel-like geometry (Figure 10). Succession A overlies Succession B with an erosional surface. Therefore, Succession A is interpreted as a channel-fill deposit.

Succession B is composed of alternating hemipelagic mudstone (Facies 1-a) and laminated fine-grained sandstone beds (Facies 2-b) (Figure 9). Walker (1985) reported that typical fine-grained turbidites can build up levees associated with a submarine channel. These turbidites were named “CCC turbidites” after their typical features: climbing-ripple, convolute laminations, and rip-up clasts. Low-density turbidites (Facies 2-b) of Succession B exhibits these characteristics (Figure 5C). There are no signs of upward thinning or thickening trends. Succession A changes gradually upward to Succession B (Figure 9), and Succession B is in turn overlain by the next Succession A section with an erosional contact. Succession B also changes abruptly to Succession A laterally, although this lateral change of lithology may be caused by a fault (Figure 9). These features of Succession B are characteristics of spill-over deposits from the channel, in which Succession A was deposited.

Based on palaeocurrent data from cross-lamination and sole marks in each succession (Figure 10), turbidites of Succession A are considered to have been transported from northwest to southeast, while those of Succession B were transported from north to south. Spill-over turbidity currents occurred oblique to the orientation of the channel (Winn & Dott, 1979).

To summarize the features described above, it is inferred that this facies association was deposited in a channel-levee complex environment. This facies association overlies flat basin plain facies associations, and it differs from the basin plain facies associations in two respects: it consists of two markedly different successions and includes large slump deposits (Facies 4 generated by submarine slope failure). The channel-levee complex and proximal basin plain facies association are inferred to have existed contemporaneously because Facies 3-a, which only occur in the proximal basin plain facies association, often contains intra-basinal clasts with features characteristic of Facies 2-b (Figure 5F), which is only observed in the channel-levee complex facies association. In addition, the submarine slope facies association overlies the channel-levee complex facies association. Therefore, this facies association probably located at the foot of the slope, which is between the slope and the most proximal side of the flat basin plain environments. It is known that channels and huge debris flow or avalanche deposits are often developed in the foot of the slope environment (Wynn *et al.*, 2000; Pickering *et al.*., 2001).

Submarine slope facies association (Kiritappu Formation)

The submarine slope facies association is composed mainly of thinly bedded sandstone beds (Facies 2-a and 2-b) and pebbly sandstone beds (Facies 3-b), together with subordinate bioturbated sandy siltstones (Facies 1-b) and pebble to cobble conglomerate beds (Facies 3-c). This facies association consists of two successions A and B, which differ in terms of facies and stacking patterns (Figure 11).

Succession A consists mainly of pebbly sandstone beds (Facies 3-b) and conglomerate beds (Facies 3-c). This succession tends to be fining upward, and its thickness varies laterally. Lateral variation of its thickness is typically observed in the 1.5 km wide outcrop of the Kiritappu Island (Figure 2, IV), where this succession shows channel-like geometry and its thickness changes 0 to more than 50 m. These features suggest that Succession A was deposited in topographical lows such as gullies or channels (Walker, 1978).

Succession B is composed of fine-grained sandstone beds (Facies 2-a and b) and sandy siltstone with slump scars (Facies 1-b). It does not show any overall grain-size trends. It is observed at the outcrop that Succession B is overlain by Succession A with an erosional surface, and conformably overlies Succession A. The good lateral continuity of beds in Succession B suggests that it was deposited in a topographically flat area such as on either side of a gully. Slump scars observed in Facies 1-b indicate deposition in a slope environment.

To summarize, the two successions are indicative of a slope environment with gullies or channels. Palaeocurrent data collected from cross-lamination and clast imbrication give an approximate flow direction towards the southeast (Figure 8).

Both the channel-levee complex and submarine slope facies associations were deposited in the environment where gullies or channels developed. The latter, however, includes more proximal (coarse-grained) sediment gravity flow deposits (Facies 3-c), that the former does not. Additionally, the presence of slump scars in the submarine slope facies association is characteristic of the most proximal area of submarine slumping (Clari & Ghibaudo, 1979). Chaotic deposits (Facies 4) in the channel-levee complex facies association generally occur distal to the region of submarine slumping (Prior *et al.*., 1984).

5. Depositional system and history

The 4 formations in the Nemuro Group exhibits successive upward-coarsening succession (Figures 3, 12). The Oborogawa Formation, which is the lowermost formation in this study area, is referred to the distal basin plain facies association. It is overlain by the proximal basin plain facies association (Hamanaka Formation). The channel-levee complex facies association (Akkeshi Formation), including the deposits of a channel-levee complex, succeeds the proximal basin plain facies association (Hamanaka Formation). Finally, the submarine slope facies association (Kiritappu Formation) caps the channel-levee complex facies association (Akkeshi Formation).

The upward-shallowing succession in the Nemuro Group is thought to have formed by the progradation of the submarine slope. Palaeocurrent data (Figure 8) indicates that the slope prograded primarily from the northwestern area of the basin. The palaeocurrent directions vary but the main trend is towards the south in the distal basin plain facies association. The proximal basin plain facies association contains sediment gravity flow deposits transported from north to south. All successions in the channel-levee complex and submarine slope facies associations exhibit northwest to southeast palaeocurrent directions. To summarize, the sediment-supply area was probably located north to northwest of the basin, although the center of the source area may have migrated from northeast to northwest. There is no indication of a southern source area as suggested by Kiminami (1983).

The enhancement of lithological variation in the Nemuro Group is due to the migration of depositional environments from the topographically flat basin plain to the submarine slope. Kiminami (1979, 1983) suggested that the Nemuro Group had two sediment-supply areas, based primarily on the grain composition of sandstone, which changes remarkably in each lithofacies. Compositional changes, however, may simply reflect grain size differences between facies. Korsch (1993) showed that the chemical composition of sandstone changes readily with grain size even within a single graded turbidite bed.

6. Tectonic setting and cause of slope progradation

Strata formed by the progradation of the slope, with extensive accumulations of sediment gravity flow deposits in the lower part, are common in tectonically active areas such as colliding volcanic arcs (e.g., Ito & Masuda, 1988). The Nemuro Group is thought to have been deposited in a tectonically active area, and the source area of the group has been inferred as part of a volcanic arc that existed from the Late Cretaceous to the Paleocene. The abundance of immature volcanic rock fragments in sandstones of the group (Kiminami, 1979, 1983; Ogasawara *et al.*., 1998) supports this view. Therefore, it may represent a forearc basin deposit leading a northern volcanic arc.

There are several possible scenarios for the tectonic evolution of the Kuril Arc. Kimura (1986) interpreted the hiatus within the Kuril Arc in the Eocene as attributable to ridge subduction beneath the Kuril Arc. The results of the present study, however, imply that regression began in the Early Maastrichtian, and as such was not a sudden event. However, it is difficult to determine the reason for the regression.

One possible explanation for the slope progradation recorded by the Nemuro Group is the potential increase in sediment supply due to igneous activity along the Kuril Arc. Generally, rapid increases in sediment supply render submarine slopes steep and unstable (Walker, 1992). As a result, the slope progrades with large-scale avalanching (Prior *et al.*., 1984). The Hamanaka Formation is intruded by several mafic igneous rock sills dated at about 70 Ma (Shibata, 1985). Ogasawara *et al.*. (1998) estimated that the igneous activity in the source area of the Nemuro Group lasted until 54 Ma according to compositional analysis and K-Ar dating of clasts. Therefore, submarine slope progradation is thought to have occurred almost contemporaneously with igneous activity in the source area in the Nemuro Group during the late Maastrichtian to Paleocene. It is possible that igneous activity in the palaeo-Kuril Arc generated large amounts of sediment and caused the progradation of the submarine slope.

A second possibility, however, is that a eustatic sea-level lowering initiated slope progradation. It is known that a eustatic sea-level fall occurred during the middle Campanian - Thanetian (Haq *et al.*., 1988) broadly coeval with deposition of the Nemuro Group (Naruse *et al.*., 2000). Such a drop in sea level may have caused progradation of the depocenter on the shelf, resulting in the supply of enormous sediment loads to the feeder channel of the turbidite system. For example, Sakai and Masuda (1997) suggested that a turbidite system in the Pliocene-Pleistocene Kakegawa Group in central Japan was activated by a eustatic sea-level fall. Weimer (1989) also suggested that mass transport complexes initiated new phases of the Mississippi submarine fan during lowering of relative sea level, slumping on the slope, and canyon formation.

7. Conclusion

An overall regressive trend has been documented based on depositional facies analysis in the Upper Cretaceous - Paleogene Nemuro Group, in eastern Hokkaido, northern Japan. The lowermost Oborogawa Formation was deposited in a distal basin plain, the succeeding Hamanaka Formation in a proximal basin plain, the Akkeshi Formation on the channel-levee complex, and the uppermost Kiritappu Formation on the submarine slope. Palaeocurrent data indicate that the deposits of the Nemuro Group were transported from the north/northwest towards the south and southeast. Hence, the Nemuro Group in this study area is concluded to have been deposited by slope progradation away from a northern source area. This study has also indicated that regression in the Kuril Arc began as early as Maastrichtian. This may have been induced by volcanic activity along the Kuril Arc or a significant eustatic fall in sea level.

Acknowledgements

I sincerely thank many people in the Department of Geology & Mineralogy, Kyoto University, in particular Dr Haruyoshi Maeda for his guidance throughout my study, and Prof. Fujio Masuda and Dr Tetsuya Sakai for their helpful discussion and advice. I am also greatly indebted to the Kiritappuri guest-house, the Kiritappu Marsh Centre, the Akkeshi Marine Biological Station, and the Akkeshi Marine Memorial Center, who encouraged me during my field work.

References

Allen, J. R. L. 1971. Instantaneous sediment deposition rates deduced from climbing-ripple cross-lamination: *Journal of the Geological Society, London* **127**, 553-561.

Bagnold, R. A. 1954. Experiments on a gravity-free dispersion of large solid spheres in a Newtonian fluid under shear.

Proceedings of the Royal Society of London, Series A **225**, 49-63.

Bouma, A. H. 1962. *Sedimentology of some flysch deposits*, 168 pp. (Elsevier, Amsterdam).

Clari, P. & Ghibaudo, G. 1979. Multiple slump scars in the Tortonian type area (Piedmont Basin, northwestern Italy). *Sedimentology* **26**, 719-730.

Endo, N. & Masuda, F. 1997. Small ripples in dunes regime and interpretation about dunes-missing in turbidites. *Journal of the Geological Society of Japan* **103**, 741-746.

Haq, B. U., Hardenbol, J. & Vail, P. R. 1988. Mesozoic and Cenozoic chronostratigraphy and cycles of sea-level change. In *Sea-level changes: an integrated approach* (eds Wilgus, C. K., Hastings, B. S., Kendall, C. G.., Posamentier, H. W., Ross, C. A. & Van Wagoner, J. C.), pp. 71-108 (SEPM, Society for Sedimentary Geology, Tulsa, OK).

Hiscott, R. N., Middleton, G. V. 1979. Depositional mechanics of thick-bedded sandstones at the base of a submarine slope, Tourelle Formation (Lower Ordovician), Quebec, Canada. In *Geology of continental slopes* (eds Doyle, L. J., Pilkey, O. H.), pp. 307-326 (SEPM, Society for Sedimentary Geology, Tulsa, OK).

Ito, M. & Masuda, F. 1987. Late Cenozoic deep-sea to fan-delta sedimentation in an arc-arc collision zone, central Honshu, Japan: sedimentary response to varying plate-tectonic regime. In *Fan deltas: sedimentology and tectonic settings* (eds Nemec, W. & Steel, R. J.), pp. 400-418 (Blackie and Son. Glasgow.).

Johnson, A. M. 1970. *Physical processes in geology; a method for interpretation of natural phenomena; intrusions in igneous rocks, fractures and folds, flow of debris and ice*, 577 pp. (Freeman, San Francisco).

Kiminami, K. 1978. Stratigraphic re-examination of the Nemuro Group. *Chikyu-Kagaku* (*Earth Sciences*) **32**, 120-132.

Kiminami, K. 1979. Sedimentary petrography of the Nemuro Group.

Chikyu Kagaku (*Earth Sciences*) **33**, 152-162.

Kiminami, K. 1983. Sedimentary history of the Late Cretaceous-Paleocene Nemuro Group, Hokkaido, Japan: a forearc basin of the Paleo-Kuril arc-trench system. *Journal of Geological Society of Japan* **89**, 607-624.

Kimura, G. & Tamaki, K. 1986. Tectonic framework of the Kuril Arc since its initiation. In *Advances in earth and planetary sciences; formation of active ocean margins* (eds Nasu, N., Kobayashi, K., Uyeda, S., Kushiro, I. & Kagami, H), pp. 641-676 (Terra Science Publish Co., Tokyo, Japan).

Kneller, B. & Buckee, C. 2000. The structure and fluid mechanics of turbidity currents: a review of some recent studies and their geological implications. *Sedimentology* **47**, 62-94.

Korsch, R. J., Roser, B. P. & Kamprad, J. L. 1993. Geochemical, petrographic and grain-size variations within single turbidite beds. *Sedimentary Geology* **83**, 15-35.

Kusunoki, K. & Kimura, G. 1998. Collision and extrusion at the

Kuril-Japan arc junction. *Tectonics* **17**, 843-858.

Lowe, D. R. 1979. Sediment gravity flows: their classification and some problems of application to natural flows and deposits. *Society of Economic Palaeontologists and mineralogists, Special Publication* **27**, 75-82.

Lowe, D. R. 1982. Sediment gravity flows: II. Depositional models with special reference to the deposits of high-density turbidity currents. *Journal of Sedimentary Petrology* **52**, 279-297.

Middleton, G. V. & Hampton, M. A. 1976. Subaqueous sediment transport and deposition by sediment grabity flows. In *Marine sediment transport and environmental management* (eds Stanley, D. J. & Swift, D. J. P.), pp. 197-218 (Wiley, New York).

Mulder, T. & Alexander, J. 2001. The physical character of subaqueous sedimentary density flows and their deposits. *Sedimentology* **48**, 269-299.

Nagao, S. 1957. The Cretaceous system in the eastern part of

Hokkaido. *Kenkyurenrakushi of the Japanese Upper Cretaceous Systems* **5**, 43-46.

Naruse, H., Maeda, H. & Shigeta, Y. 2000. Newly discovered Late Cretaceous molluscan fossils and inferred K/T boundary in the Nemuro Group, eastern Hokkaido, northern Japan. *Journal of Geological Society of Japan* **106**, 161-164.

Ogasawara, M., Shibata, K. & Uchiumi, S. 1998. K-Ar ages and petrological characteristics of granitoid pebbles from the Eocene Beppo Formation in the Kushiro region, Hokkaido, Japan. *Journal of Geological Society of Japan* **104**, 516-524.

Okada, H., Yamada, M., Matsuoka, H., Murota, T. & Isobe, T. 1987. Calcareous nannofossils and biostratigraphy of the Upper Cretaceous and lower Paleogene Nemuro Group, eastern Hokkaido, Japan. *Journal of the Geological Society of Japan* **93**, 329-348.

Pickering, K. T., Hiscott, R. N. & Hein, F. J. 1989. *Deep marine environments: clastic sedimentation and tectonics*, 416 pp. (Unwin Hyman, London).

Pickering, K. T., Hodgson, D. M., Platzman, E., Clark, J. D. & Stephens, C. 2001. A new type of bedform produced by backfilling processes in a submarine channel, Late Miocene, Tabernas-Sorbas basin, SE Spain. *Journal of Sedimentary Research* **71**, 692-704.

Postma, G.. 1984. Mass-flow conglomerates in a submarine canyon: Abrioja fan-delta, Pliocene, southeast Spain. In *Sedimentology of gravels and conglomerates* (eds Koster, E. H. & Steel, R. J.), pp. 237-258 (Canadian Society of Petroleum Geologists. Calgary, AB, Canada.).

Prior, D. B., Bornhold, B. D. & Johns, M. W. 1984. Depositional characteristics of a submarine debris flow. *Journal of Geology* **92**, 707-727.

Sakai, T. & Masuda, F. 1997. Slope turbidite packets in a fore-arc basin fill sequence of the Plio-Pleistocene Kakegawa Group; their formation and sea-level changes; discussion and reply. *Sedimentary Geology* **112**, 297-304.

Sanders, J. E. 1965. Primary sedimentary structures formed by turbidity currents and related resedimentation mechanisms. *Society of Economic Palaeontologists and mineralogists, Special Publication* **12**, 192-219

Shanmugam, G. 1996. High-density turbidity currents: are they sandy debris flows? *Journal of Sedimentary Research* **66**, 2-10.

Shibata, K. 1985. Isotopic dating of alkali rocks in the Late Cretaceous Nemuro Group from Hokkaido, Japan. In *Bulletin of Liaison and Informations, IGCP Project 196, Calibration of the Phanerozoic Time Scale*. p. 20 (International Geological Correlation Programme).

Sohn, Y. K. 1997. On traction-carpet sedimentation. *Journal of Sedimentary Research* **67**, 502-509.

Takahashi, T. 2001. Mechanics and simulation of snow avalanches, pyroclastic flows and debris flows. In *Particulate gravity currents* (eds McCaffrey, W. D., Kneller, B. C. & Peakall, J.), pp. 11-43 (Blackwell Science, Oxford).

Walker, R. G. 1978. Deep-water sandstone facies and ancient submarine fans: models for exploration for stratigraphic traps. *American Association of Petroleum Geologists Bulletin* **62**, 932-966.

Walker, R. G. 1985. Mudstones and thin-bedded turbidites associated with the Upper Cretaceous Wheeler Gorge conglomerates, California: a possible channel-levee complex. *Journal of Sedimentary Petrology* **55**, 279-290.

Walker, R. G. 1992. Turbidites and submarine fans. In *Facies models, response to sea level change* (eds Walker, R.G. & James, N.P.), Geological Association of Canada, pp. 239-263 (Geological Association of Canada. St. Johns, NF, Canada.)

Weimer, P. 1989. Sequence stratigraphy of the Mississippi Fan (Plio-Pleistocene), Gulf of Mexico. *Geo-Marine Letters* **9**, 185-272.

Winn, R. D. & Dott, R. H. Jr 1979. Deep-water fan-channel conglomerates of Late Cretaceous age, southern Chile.

Sedimentology **26**, 203-228.

Wynn, R. D., Masson, D. G., Stow, D. A. V. & Weaver, P. P. E. 2000. The Northwest African slope apron; a modern analogue for deep-water systems with complex seafloor topography. *Marine and Petroleum Geology* **17**, 253-265.

Yoshida, S. 1967. Planktonic foraminifera from the Paleocene Kiritappu Formation and its biostratigraphic significance. In *Contributions to celebrate Prof. Ichiro Hayasaka's 76th Birthday* (eds Prof Ichiro Hayasaka's 76th Birthday Memorial Project Committee), pp. 85-90 (Hashimotokakubundo, Japan).

Figure Captions

Figure 1. Distribution of the Nemuro Group and location of the study areas. Modified after Kusunoki & Kimura (1998). A, arc-arc junctions around the Japanese Islands. B, distribution of the Nemuro Group. C, location of the study areas. I, Eastern Nemuro area; II, Western Nemuro Area; III, Hamanaka area; IV, Kiritappu area.

Figure 2. Geological maps of the study-areas; for locations, see Figure 1C. Columnar sections of localities H1-3, A1-6 and K1-3 are respectively shown in Figures 6, 8 and 10.

Figure 3. Lithostratigraphic subdivision of the Nemuro Group in the Nemuro area. Lithologies and their interpretations of depositional environments are discussed in the text.

Figure 4. Depositional facies of the Nemuro Group. Facies 1-a and 1-b are composed of mudstone and other facies are composed of sandstone and conglomerate; see text for details.

Figure 5. Field photographs. A, slump scar observed in mudstone (Facies 1-b) of the Kiritappu Formation; white arrows indicate erosional surface. B, thinly bedded fine sandstone (Facies 2-a) in the Hamanaka Formation. C, thinly bedded laminated sandstone (Facies 2-b) in the Akkeshi Formation. D, flute casts on the base of sandstone bed (Facies 2-b) in the Akkeshi Formation; the bed is overturned because of slump folding. E, structureless coarse sandstone in the Hamanaka sandstone; the hammer indicates the boundary between divisions 1 (inverse graded) and 2 (structureless), and a white arrow indicates mud clasts included in structureless sandstone. F, intra-basinal clast included in a structureless coarse sandstone bed (Facies 3-a) of the Hamanaka Formation; the clast is composed of laminated fine sandstone (Facies 2-b).

Figure 6. Field Photographs. A, thickly bedded pebbly sandstone in the Akkeshi Formation; scale bar represents 2 m. B, cross-stratification observed in pebbly sandstone (Facies

3-b) of the Akkeshi Formation; scale bar represents 20 cm. C, conglomerate (Facies 3-c) in the Kiritappu Formation; ruler is 1 m long. D, chaotic deposits in the Akkeshi Formation; deformed sedimentary rock blocks are scattered in pebbly mudstone matrix; ruler is 1 m long.

Figure 7. Columnar sections from the localities H1-3 in the Hamanaka Formation. Each localities are correlated by tuff beds. Lateral correlation of tuff beds and sandstone beds are indicated by solid and dashed lines respectively. Localities H1-3 are shown in Figure 2.

Figure 8. Rose diagrams summarizing palaeocurrent and slump fold data from the Hamanaka, Akkeshi and Kiritappu formations.

Figure 9. Columnar sections from the localities A1-6 in the Akkeshi Formation. Wavy line exhibits observed erosional base of Succession A, and dashed line indicates possible erosional base. Localities A1-6 are shown in Figure 2. Each sections are arranged based on the assumption that there are no large faults

in gaps of the outcrops because faults are rare in this area and each localities are very close.

Figure 10. Distribution of successions A and B of the channel-levee complex facies association. Rose diagrams indicate palaeocurrent data of each successions. Strikes and dips of Succession A show gradual change laterally and suggest its channel-like geometry. Those of Succession B are similar to general trend of the Nemuro Group in this area. Localities A1-6 are shown in Figure 2. Lower right illustration is a schematic reconstruction model for depositional environments of successions A and B.

Figure 11. Columnar sections from the localities K1-3 in the Kiritappu Formation. Dashed line indicates an erosive base of the conglomerate bed. Localities K1-3 are in the single 1.6 km wide outcrop, and their locations are shown in Figure 2.

Figure 12. Facies associations and schematic reconstruction of depositional environments of the Nemuro Group.

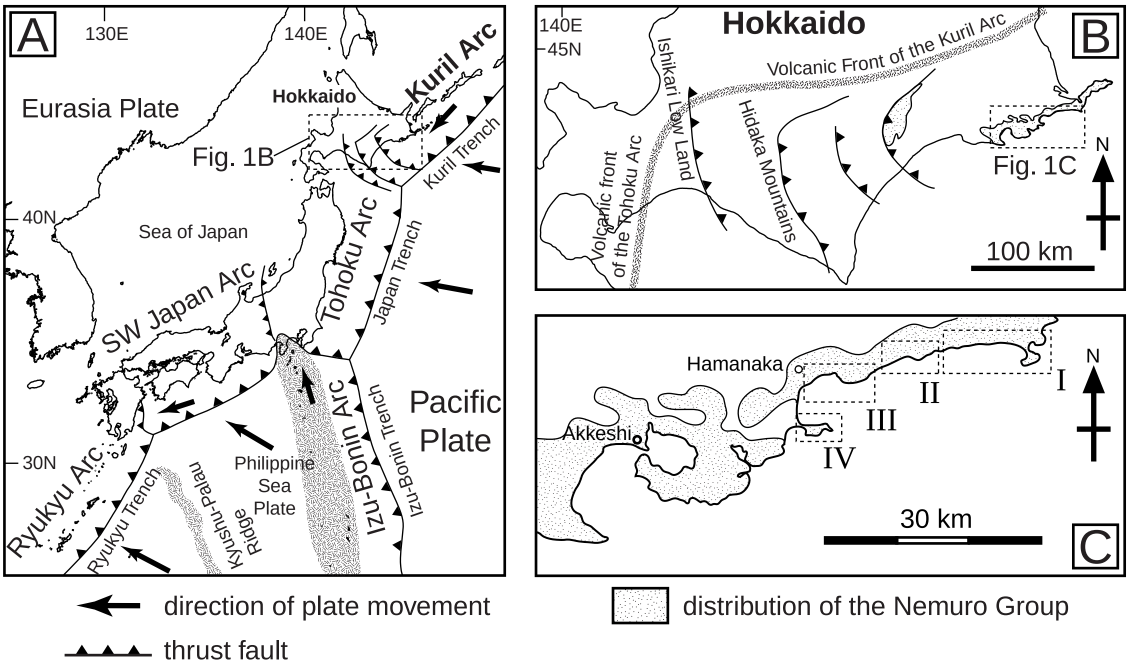
A
130E
140E
Eurasia Plate
Hokkaido
Kuril Arc
Fig. 1B
Kuril Trench
40N
Sea of Japan
Tohoku Arc
Japan Trench
SW Japan Arc
Pacific Plate
30N
Ryukyu Arc
Ryukyu Trench
Kyushu-Palau Ridge
Philippine Sea Plate
Izu-Bonin Arc
Izu-Bonin Trench
B
140E
45N
Hokkaido
Volcanic Front of the Kuril Arc
Ishikari Low Land
Hidaka Mountains
Volcanic front of the Tohoku Arc
Fig. 1C
N
100 km
C
Hamanaka
Akkeshi
I
II
III
IV
N
30 km
direction of plate movement
thrust fault
distribution of the Nemuro Group

Figure 1

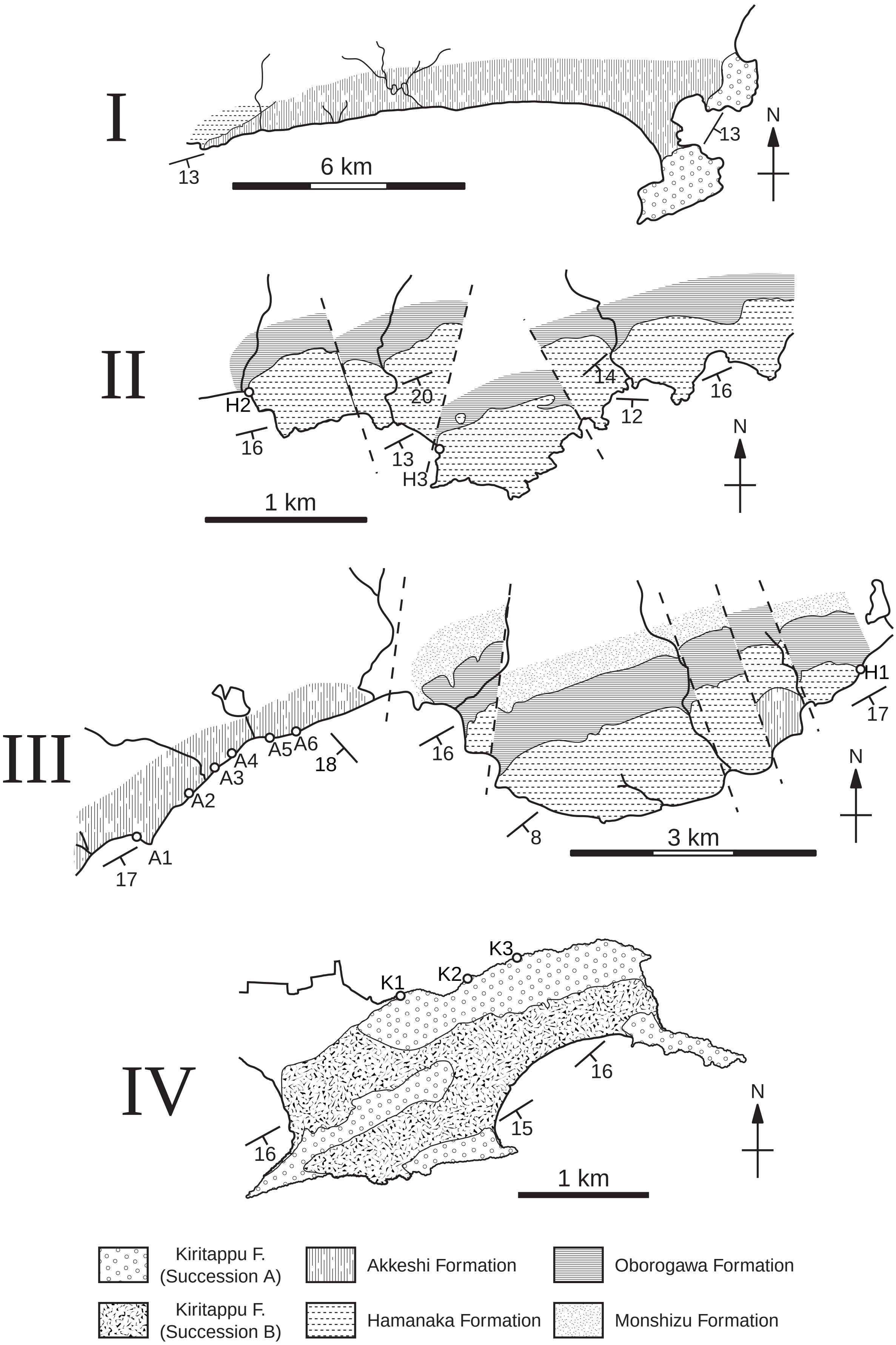

I
13
13
6 km
N
II
H2
H3
20
16
13
14
12
16
1 km
N
III
A1
A2
A3
A4
A5
A6
H1
17
18
16
8
17
3 km
N
IV
K1
K2
K3
16
15
16
1 km
N
Kiritappu F. (Succession A)
Kiritappu F. (Succession B)
Akkeshi Formation
Hamanaka Formation
Oborogawa Formation
Monshizu Formation

Figure 2

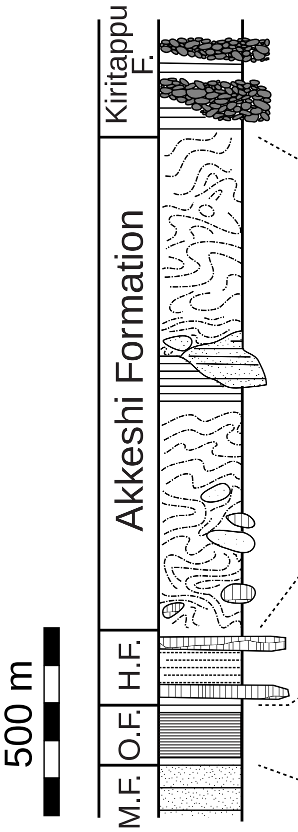

Lithology	Depositional Environment
Conglomerate (Facies 3-c) Sandy siltsone with slump scars (Facies 1-b)	Upper slope Submarine channels and slump scars are developed
Chaotic deposits (Facies 4) Alternating beds of thin-bedded sandstone (Facies 2-b) and mudstone (Facies 1-a) Thick-bedded pebbly sandstone (Facies 3-b)	Channel-levee complex Slump deposits and channel-levee complex
Alternating beds of mudstone (Facies 1-a) and thick-bedded sandstone (Facies 3-a) or thin-bedded sandstone (Facies 2-a)	Proximal basin plain Proximal turbidites and hemipelagic mudstone
Alternating beds of mudstone (Facies 1-a) and thin-bedded sandstone (Facies 2-a) Mudstone (Facies 1-a)	Distal basin plain Distal turbidites and hemipelagic mudstones

M.F., Monshizu Formation; O.F. Oborogawa Formation; H. F., Hamanaka Formation

Figure 3

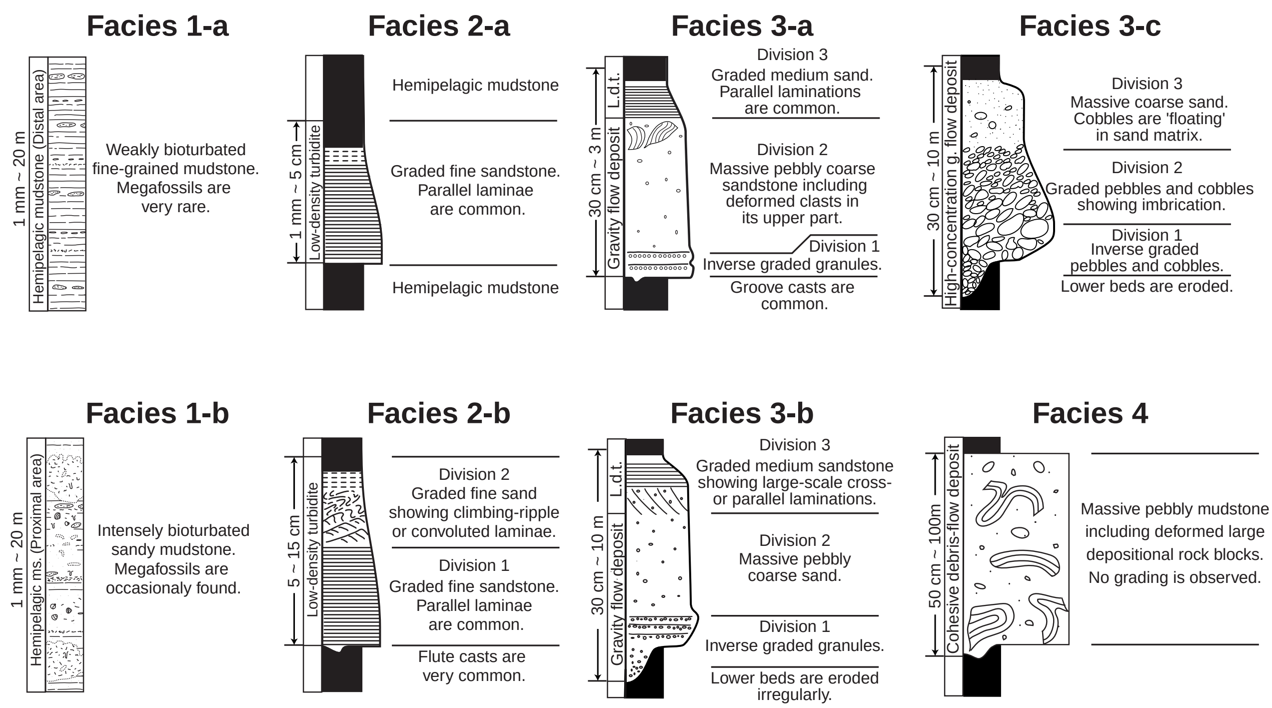
Facies 1-a
1 mm ~ 20 m
Hemipelagic mudstone (Distal area)
Weakly bioturbated fine-grained mudstone. Megafossils are very rare.
Facies 2-a
1 mm ~ 5 cm
Low-density turbidite
Hemipelagic mudstone
Graded fine sandstone. Parallel laminae are common.
Hemipelagic mudstone
Facies 3-a
30 cm ~ 3 m
Gravity flow deposit
L.d.t.
Division 3
Graded medium sand. Parallel laminations are common.
Division 2
Massive pebbly coarse sandstone including deformed clasts in its upper part.
Division 1
Inverse graded granules.
Groove casts are common.
Facies 3-c
30 cm ~ 10 m
High-concentration g. flow deposit
Division 3
Massive coarse sand. Cobbles are 'floating' in sand matrix.
Division 2
Graded pebbles and cobbles showing imbrication.
Division 1
Inverse graded pebbles and cobbles.
Lower beds are eroded.
Facies 1-b
1 mm ~ 20 m
Hemipelagic ms. (Proximal area)
Intensely bioturbated sandy mudstone. Megafossils are occasionaly found.
Facies 2-b
5 ~ 15 cm
Low-density turbidite
Division 2
Graded fine sand showing climbing-ripple or convoluted laminae.
Division 1
Graded fine sandstone. Parallel laminae are common.
Flute casts are very common.
Facies 3-b
30 cm ~ 10 m
Gravity flow deposit
L.d.t.
Division 3
Graded medium sandstone showing large-scale cross- or parallel laminations.
Division 2
Massive pebbly coarse sand.
Division 1
Inverse graded granules.
Lower beds are eroded irregularly.
Facies 4
50 cm ~ 100m
Cohesive debris-flow deposit
Massive pebbly mudstone including deformed large depositional rock blocks. No grading is observed.

Figure 4

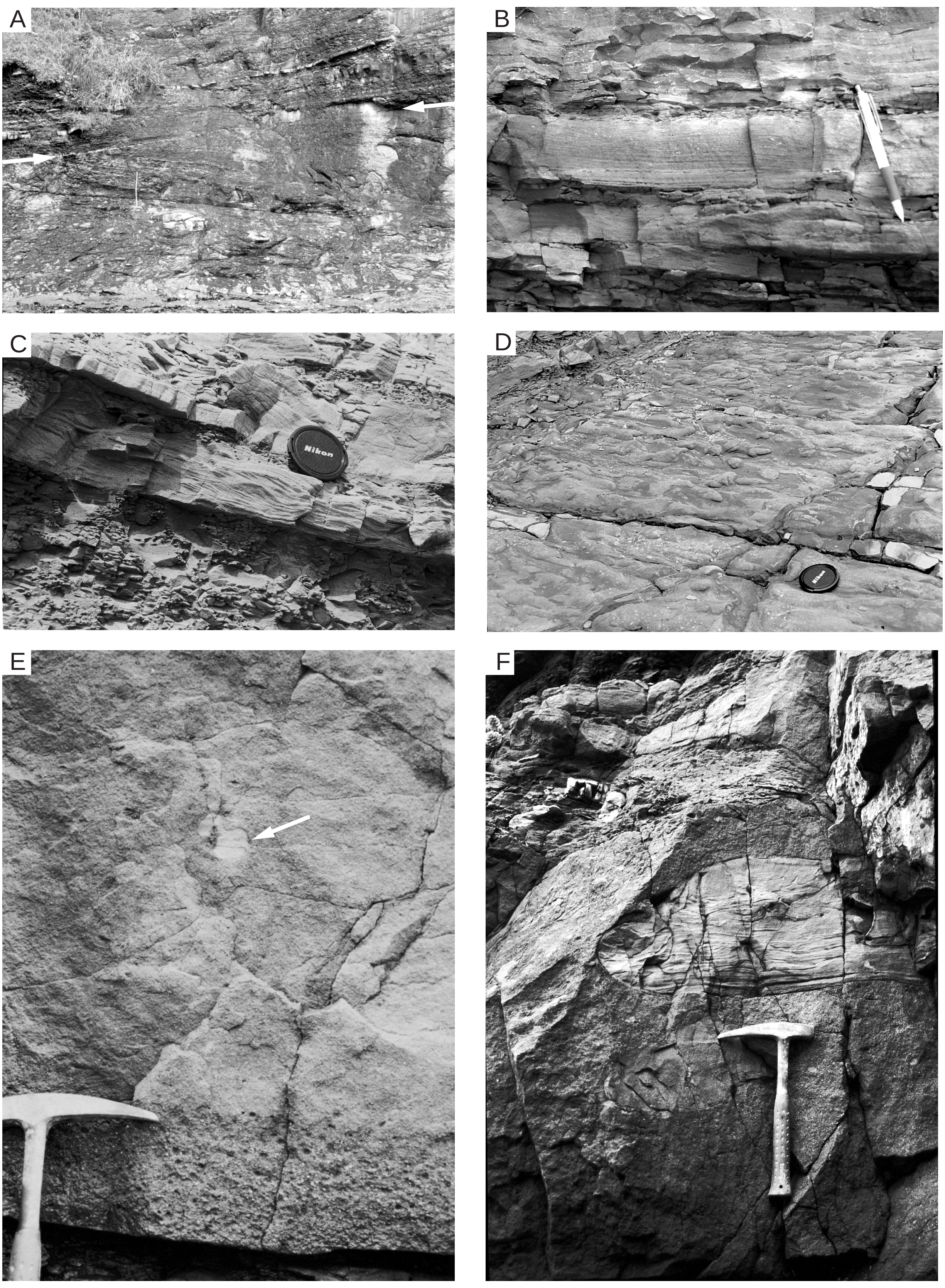

Figure 5

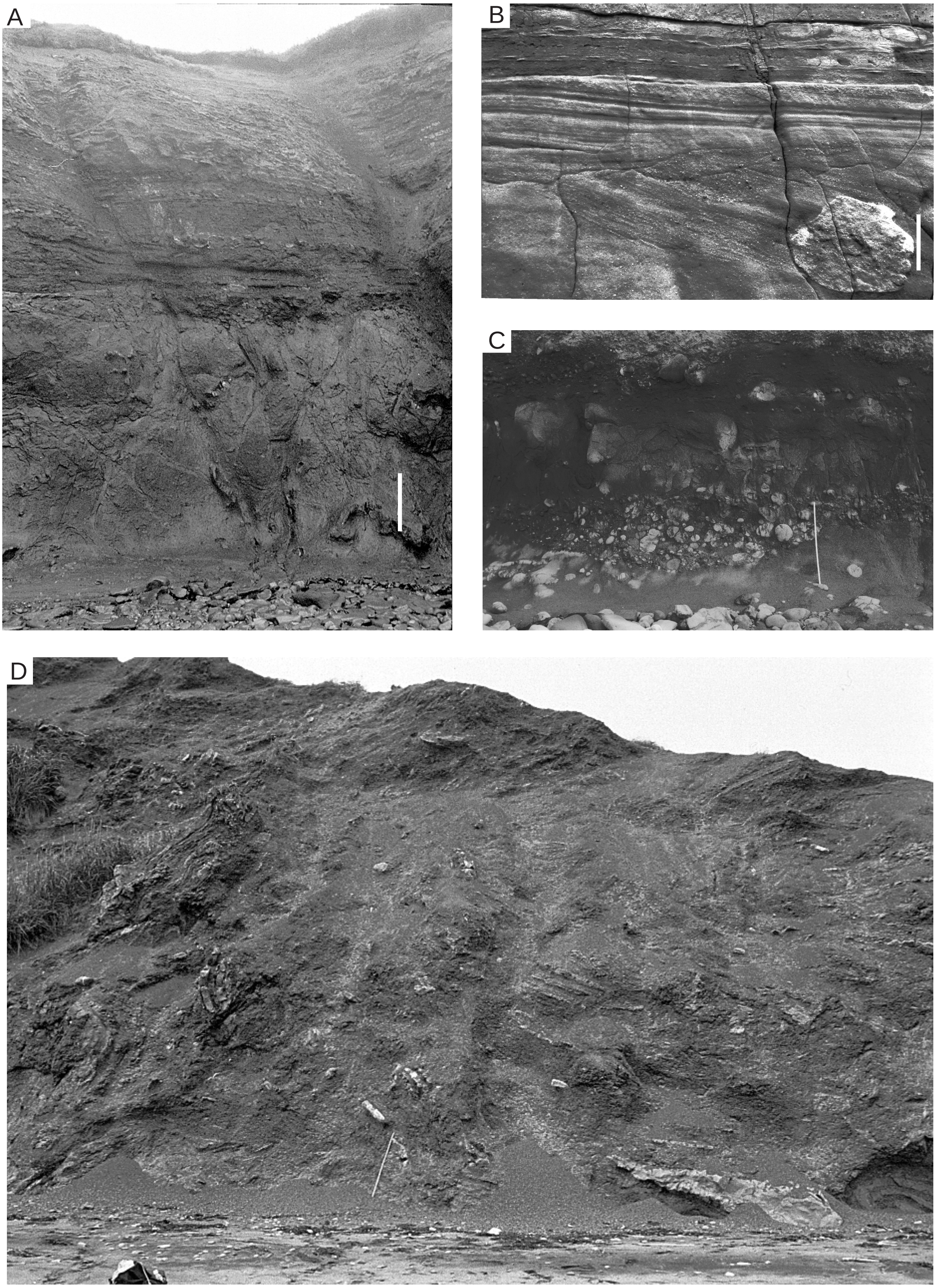

Figure 6

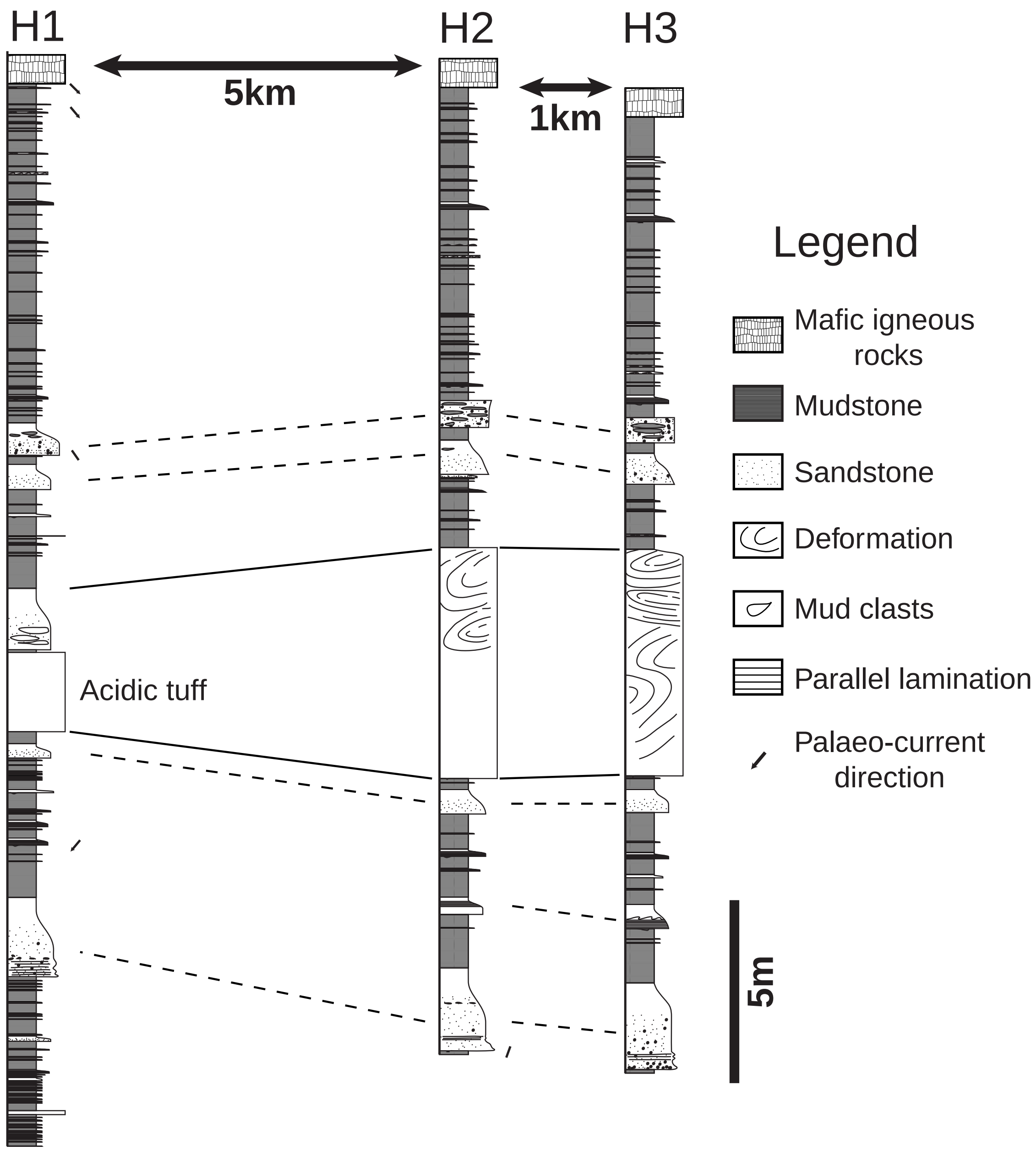

H1
H2
H3
5km
1km
Acidic tuff
Legend
Mafic igneous rocks
Mudstone
Sandstone
Deformation
Mud clasts
Parallel lamination
Palaeo-current direction
5m

Figure 7

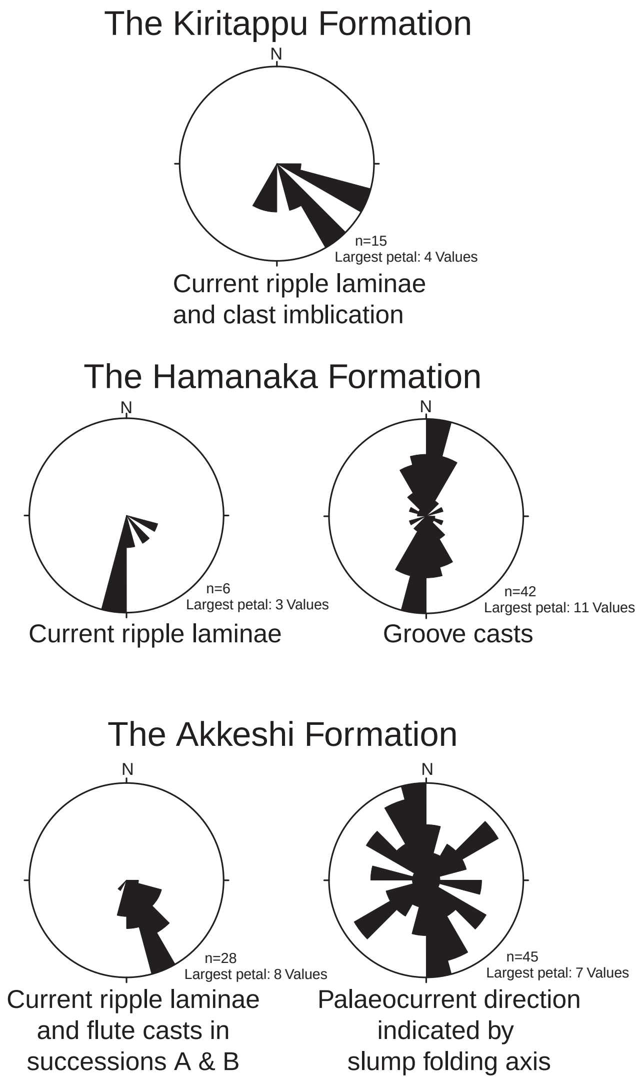

The Kiritappu Formation
N
n=15
Largest petal: 4 Values
Current ripple laminae
and clast imblication
The Hamanaka Formation
N
n=6
Largest petal: 3 Values
Current ripple laminae
N
n=42
Largest petal: 11 Values
Groove casts
The Akkeshi Formation
N
n=28
Largest petal: 8 Values
Current ripple laminae
and flute casts in
successions A & B
N
n=45
Largest petal: 7 Values
Palaeocurrent direction
indicated by
slump folding axis

Figure 8

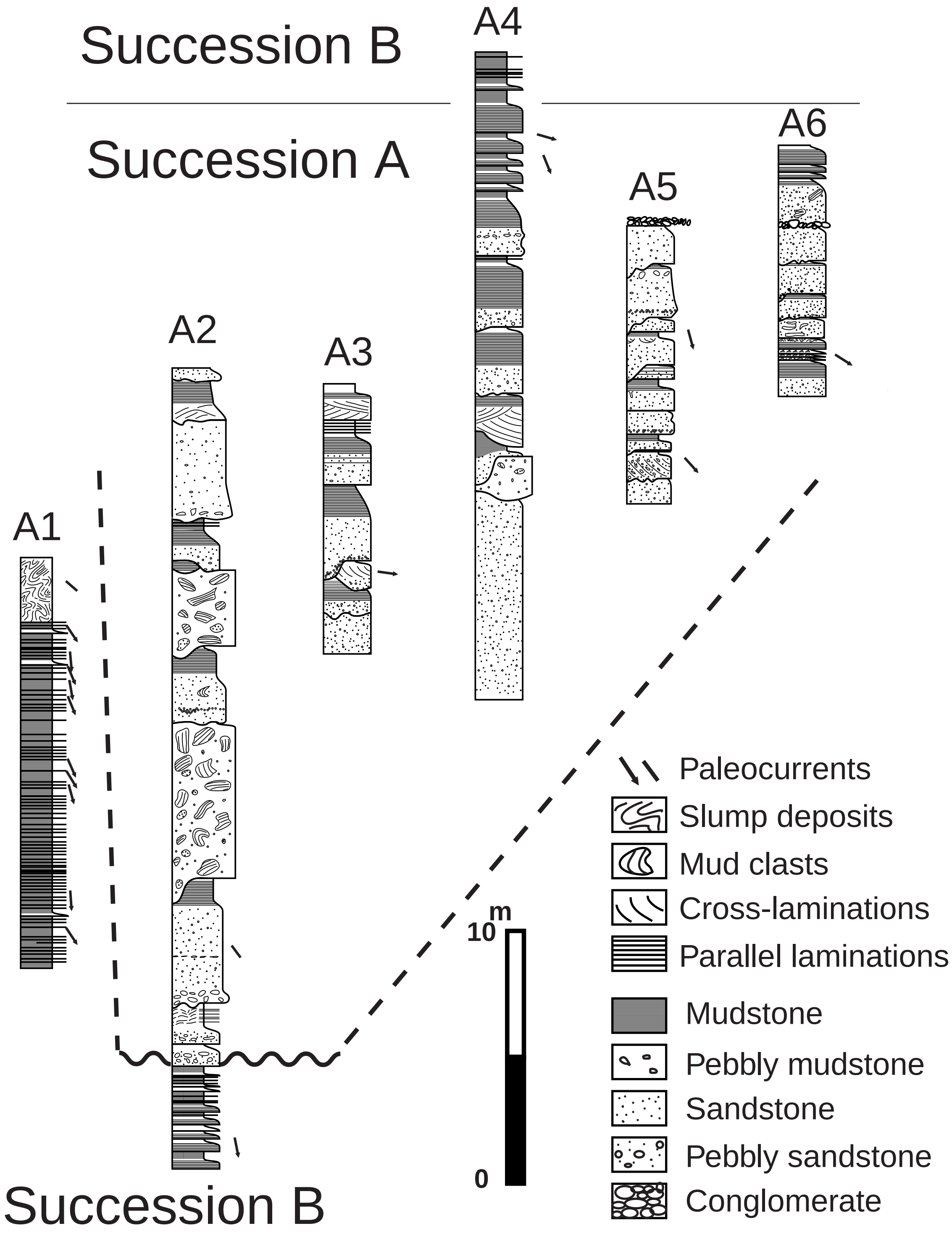

Succession B
Succession A
A1
A2
A3
A4
A5
A6
Succession B
m
10
0
Paleocurrents
Slump deposits
Mud clasts
Cross-laminations
Parallel laminations
Mudstone
Pebbly mudstone
Sandstone
Pebbly sandstone
Conglomerate

Figure 9

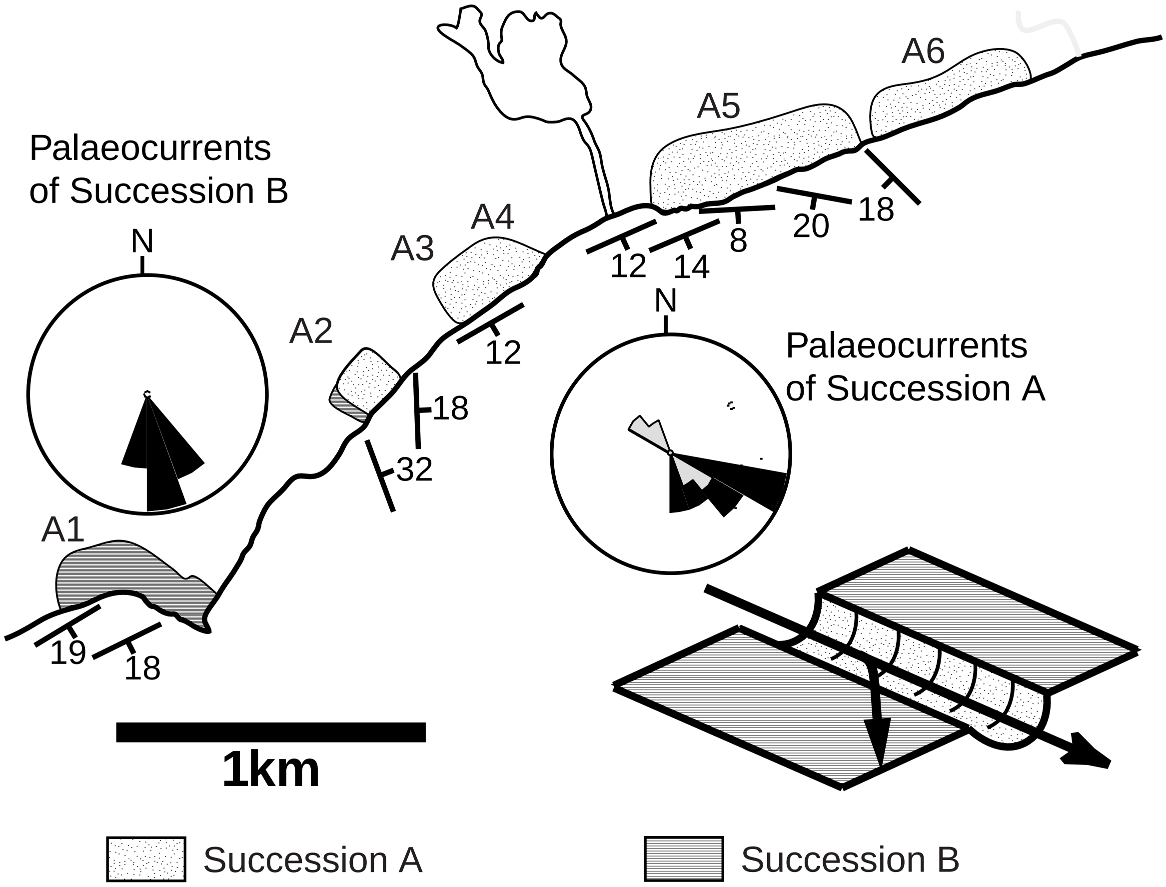
Palaeocurrents
of Succession B
N
A1
19
18
A2
A3
A4
12
18
32
12
14
8
20
18
A5
A6
N
Palaeocurrents
of Succession A
1km
Succession A
Succession B

Figure 10

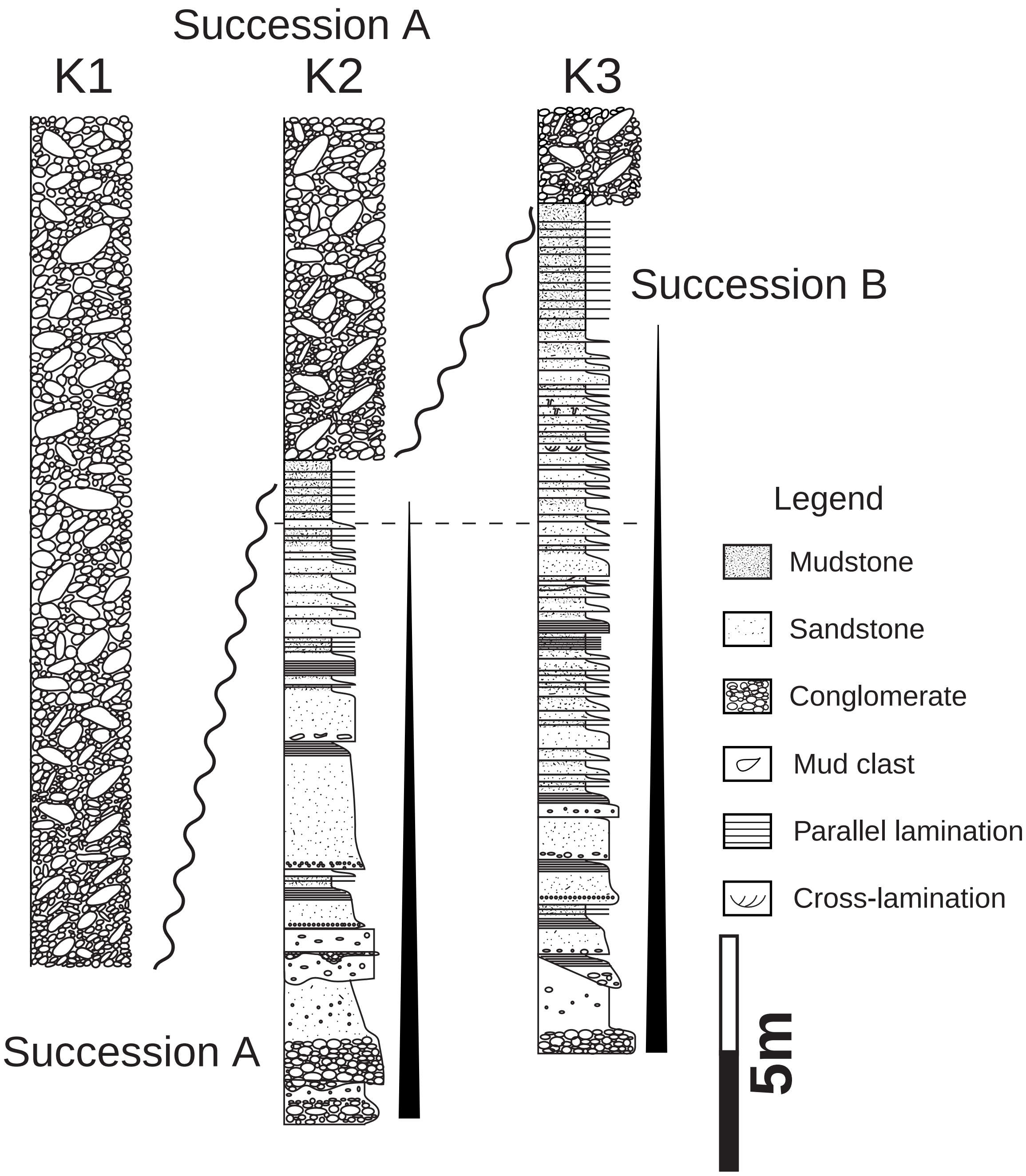

Succession A
K1
K2
K3
Succession B
Legend
Mudstone
Sandstone
Conglomerate
Mud clast
Parallel lamination
Cross-lamination
Succession A
5m

Figure 11

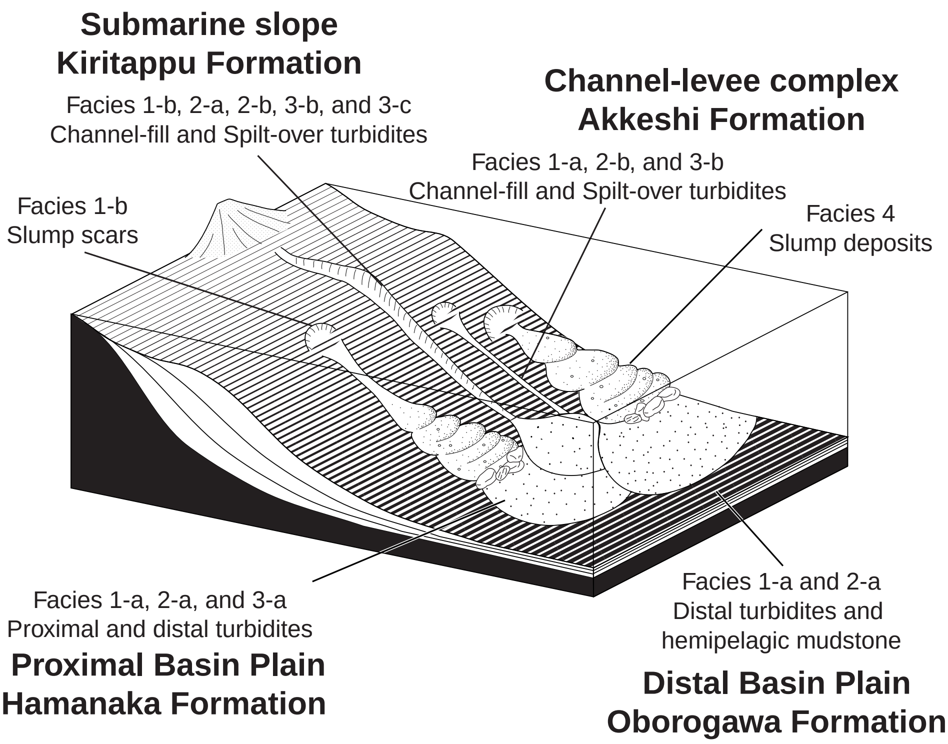
Submarine slope
Kiritappu Formation
Facies 1-b, 2-a, 2-b, 3-b, and 3-c
Channel-fill and Spilt-over turbidites
Channel-levee complex
Akkeshi Formation
Facies 1-a, 2-b, and 3-b
Channel-fill and Spilt-over turbidites
Facies 1-b
Slump scars
Facies 4
Slump deposits
Facies 1-a and 2-a
Distal turbidites and
hemipelagic mudstone
Facies 1-a, 2-a, and 3-a
Proximal and distal turbidites
Proximal Basin Plain
Hamanaka Formation
Distal Basin Plain
Oborogawa Formation

Figure 12